Journal of Horticultural Science & Biotechnology (2014) **89** (1) 61–68

Characterisation of calcium crystals in *Abelia* spp. using X-ray diffraction and electron microscopy

By GIANLUCA BURCHI[1], GARY R. BAUCHAN[2], CHARLES MURPHY[2] and MARK S. ROH[3]*
[1]Consiglio per la Ricerca e la Sperimentazione in Agricoltura, CRA-VIV Landscaping Plants and Nursery Research Unit, Via dei Fiori 8, 51012 Pescia (PT), Italy
[2]USDA, ARS, Electron and Confocal Microscope Unit, Soybean Genomics and Improvement Laboratory, B-012, 10300 Baltimore Ave., Beltsville, MD 20705-2350, USA
[3]USDA, ARS, USNA, Floral and Nursery Plants Research Unit, B-010A, 10300 Baltimore Ave., Beltsville, MD 20705-2350, USA
(e-mail: marksroh@gmail.com)
(Accepted 13 May 2013)

SUMMARY
The localisation, chemical composition, and morphology of calcium (Ca) oxalate crystals in the leaves and stems of *Abelia mosanensis* and of *A.* × *grandiflora* were analysed using a variable pressure-scanning electron microscope (VP-SEM) equipped with an X-ray diffraction system, a low temperature SEM (LT-SEM), and a transmission electron microscope (TEM). Foliar analyses of macro- and micro-elements were performed on the leaves and stems of *A. mosanensis*. A greater number of Ca oxalate crystals were observed in *A. mosanensis* than in *A.* × *grandiflora*. Three morphologically distinguishable types of crystals were observed: the prismatic crystals found inside the chloroplast, multifaceted star-like spherical and bladed aggregate crystals (druses) inside the vacuoles of the mesophyll cells, and small angular crystals (sand crystals) inside the cuticle. Semi-solid crystals that may drip and accumulate to become a solid Ca oxalate crystal were observed by LT-SEM, which indicated the growth of druses of Ca oxalate crystals. The growth of prismatic crystals and of druses were evident through the formation of crystalline lamellae. Micro-analysis indicated that the crystals were Ca oxalate and contained magnesium in *A. mosanensis*, or silicon in *A.* × *grandiflora*. *Abelia* stems with low foliar calcium concentrations showed no Ca oxalate crystal formation. This is the first report, to our knowledge, on the presence and possible growth of crystals of different morphologies and chemical compositions in *Abelia*.

Calcium (Ca) is generally abundant in the environment (Kirkby and Pilbeam, 1984), and the formation of Ca-salt crystals such as Ca oxalate in plants provides high-capacity calcium (Ca) regulation and protection against herbivory (Franceschi and Nakata, 2005). Ca oxalate crystals are common in many plant species (Arnott and Pautard, 1970) and have been reported in 215 plant families including members of the Cactaceae and Orchidaceae (Franceschi and Horner, 1980; Ward *et al*., 1997), and are present in flowers (Horner and Wagner, 1980), leaves (Franceschi, 1984), and stems (Doaigey, 1991).

Ca oxalate crystals are known to occur as intracellular or extracellular deposits (Franceschi and Nakata, 2005). Most studies on the formation of Ca oxalate crystals have reported a positive relationship between the Ca concentration in the growth medium and crystal production (Borchert, 1985; Franceschi, 1989; Zindler-Frank, 1975). The elemental composition of these crystals indicated that Ca oxalate and Ca sulphate occurred in almost all tissues, and that Ca sulphate-magnesium oxalate crystals occurred only in the mesophyll cells of *Acacia robeorum* Muslin (He *et al*., 2012). However, no information is available on the relationship between Ca concentrations in leaves and stems, and the presence of Ca-salt crystals in cells.

*Author for correspondence.

Ca oxalate crystals are considered to be the most commonly occurring biomineral in higher plants (Arnott, 1982; Franceschi and Horner, 1980; Franceschi and Nakata, 2005). In fact, Ca oxalate-producing plants accumulate Ca oxalate at between 3% – 80% (w/w) of their dry weight (DW; Libert and Franceschi, 1987), and up to 90% of the total Ca in the plant is in Ca oxalate crystals (Gallaher and Jones, 1976).

Ca oxalate crystals were first described in plants by Antonie van Leeuwenhoek in the late 1600's using a simple light microscope (Arnott and Pautard, 1970). A number of crystal forms have been found including block-like prismatic crystals (prismatic crystals) present as one or more crystals per cell, large and elongated rectangular styloids that occur as a single crystal in a cell, bundles of needle-shaped raphide crystals, masses of small angular crystals referred to as crystal sands (or sand crystals), and multifaceted star-like spherical and bladed aggregate crystals called druses. Ca oxalate crystals have been documented in detail using polarisation microscopy, X-ray diffraction (Frey-Wyssling, 1981), infra-red spectroscopy (Scureld *et al*., 1973), scanning electron microscopy (SEM), and more recently by transmission electron microscopy (TEM; Arnott, 1976; Arnott and Pautard, 1970; Franceschi and Horner, 1980; Franceschi and Nakata, 2005; Horner and Franceschi, 1981; Nakata, 2012).

However, to our knowledge, there have been no

reports on the presence of Ca oxalate crystals in members of the genus *Abelia* (family Caprifoliaceae), which is widely used as a deciduous ornamental shrub with fragrant flowers. *Abelia* × *grandiflora* is considered to be non-harmful to young children (Cuadra *et al*., 2012), based on the absence of Ca oxalate crystals and other toxic chemical constituents. In this paper, we have investigated and report on the localisation, chemical composition, and shape of Ca oxalate crystals in *A. mosanensis* I. C. Chung ex Nakai and in *A.* × *grandiflora* (Rovelli ex André) Rehder, analysed using a variable pressure-scanning electron microscope (VP-SEM) equipped with an X-ray diffraction system, a low temperature SEM (LT-SEM), and a TEM.

MATERIALS AND METHODS

Plant material

Nine-year old, field-grown *Abelia mosanensis* plants with 45 cm-long shoots and 13 nodes, and five-year-old pot-grown *A.* × *grandiflora* plants with 15 cm-long shoots and nine nodes were used. Shoots were harvested between 08.00 – 09.00 h, placed in distilled water and maintained at 20ºC until being sampled for microscopy in less than 2 h. Three-to-five shoots were harvested from each plant. Leaves formed at the sixth-to-seventh node in *A. mosanensis*, and leaves formed at the fourth and fifth nodes in *A.* × *grandiflora* were used for VP-SEM, LT-SEM, and TEM analysis. Single-node cuttings of *A. mosanensis* were rooted, without root-promoting hormone treatment, in an air-conditioned greenhouse (Lee and Roh, 2001) and used for micro-analysis as described below.

Variable pressure-scanning electron microscopy (VP-SEM)

An S-3700 VP-SEM (Hitachi High Technologies America, Inc., Pleasanton, CA, USA) fitted with an Oxford Instruments INCA® X-Ray Diffraction System was used. Micro-analysis was performed in cells without crystals (Ce) and on crystals (Cr) in both species. Further analyses were performed on roots, calli formed at the stem bases, and stem bases of *A. mosanensis*. Data (n = 4 for each sample) were collected with a minimum of 50,000 counts s^{-1} per sample. Carbon (C), nitrogen (N),

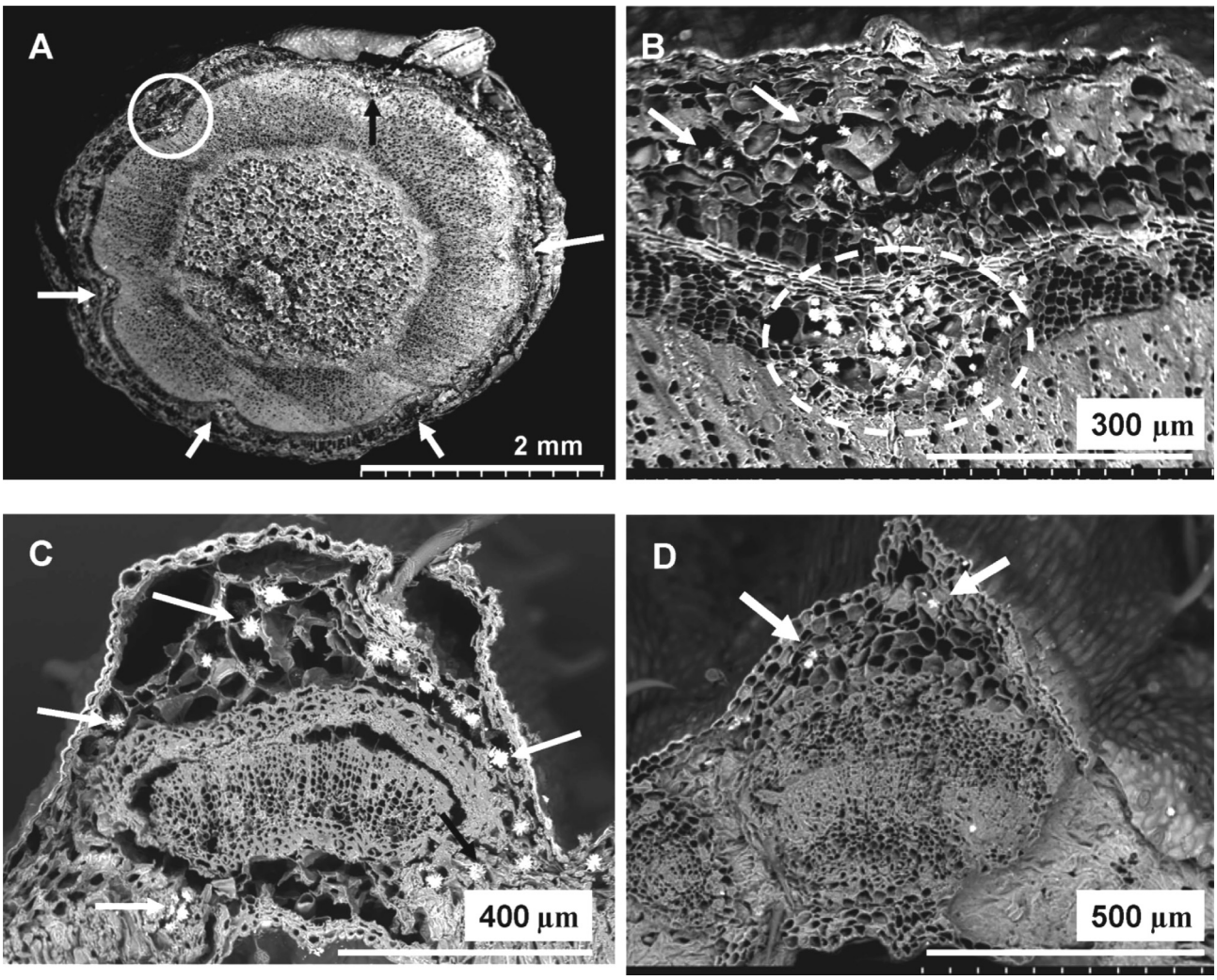

FIG. 1
Variable pressure-scanning electron microscope (VP-SEM) images of transverse sections of stems (Panels A, B) and leaves (Panel C) of *A. mosanensis*, and a leaf of *A.* × *grandiflora* (Panel D) showing druses (arrows). No druses were observed in the vascular bundles or the pith (Panel A). Numerous druses were observed in the cortical collenchyma cells in leaf traces (arrows and dotted circle; Panel B) and in mesophyll cells between the epidermis and the leaf trace in *A. mosanensis* (Panel C), and between the epidermis and the vascular bundles in the mid-vein of *A.* × *grandiflora* (Panel D). Arrows denote the locations of Ca oxalate crystals. Scale bars = 2 mm (Panel A); 300 µm (Panel B); 400 µm (Panel C); and 500 µm (Panel D).

oxygen (O), magnesium (Mg), silicon (Si), phosphorous (P), sulphur (S), chlorine (Cl), potassium (K), and Ca were analysed and the INCA® software programme was used to convert X-ray counts s^{-1} to a percentage weight after all the counting was completed.

Data were subjected to analysis of variance using SAS Software Version 9.00 (Statistical Analysis System, 2002). Means were compared by Tukey's honestly significant difference (HSD) test at $P \leq 0.01$.

Low temperature-scanning electron microscopy (LT-SEM)

Leaves and stems were sampled for observation using an S-4700 field emission scanning electron microscope (Hitachi High Technologies America, Inc.) equipped with a Quorum PP2000 cryotransfer system (Energy Beam Sciences, East Grandby, CT, USA). Samples were placed on copper plates, as described by Roh *et al.* (2012). Images were obtained using a 4pi Analysis System (Durham, NC, USA) integrated onto the SEM.

Transmission electron microscopy (TEM) of chloroplasts

Leaf tissue pieces (1 mm^2) were fixed overnight at room temperature in 2.5% (v/v) glutaraldehyde buffered with 50 mM sodium cacodylate pH 7.2 and post-fixed in 2% (v/v) osmium tetroxide buffered with 50 mM sodium cacodylate pH 7.2. Samples were dehydrated through a graded acetone series in double distilled H_2O [30 min each in 20%, 40%, 60%, 80% and 90% (v/v) acetone and three × 30 min in 100% (v/v) acetone], infiltrated with Spurr's low-viscosity embedding resin (Spurr, 1969) and acetone [4 h each in 20%, 40%, 60%, and 80%, and three × 4 h in 100% (v/v) acetone], and polymerised at 65ºC for 24 h. Thick sections (90 mm) were cut on a Reichert A/O Ultracut microtome (American Optical Co., Southbridge, MA, USA) using a diamond knife (DiATOME USA, Hatfield, PA, USA) and mounted on 400-mesh nickel grids. Sections were stained with 4% (w/v) aqueous uranyl acetate for 15 min, followed by 3% (w/v) aqueous lead citrate for 5 min. Specimens were viewed with a Hitachi HT 7700 TEM (Hitachi High Technologies America Inc., Schaumburg, IL, USA) and images were captured using an AMT XR-41C 4 megapixel camera.

Tissue analysis of macro- and micro-elements in the stems and leaves of A. mosanensis

Leaves formed at the seventh node from the proximal end of 15 – 20 shoots, and the internode subtending the leaf, were collected for macro- and micro-element analysis (tissue analysis) in triplicate (JR Peters Laboratory, Allentown, PA, USA; Roh *et al.*, 2012) on a inductively-coupled atomic emission spectrometer [(ICP)-IRIS plasma spectrometer; Thermo Jarrell Ash Corp., Franklin, MA, USA]. Only the data for K, Ca, and Mg concentrations are presented. Data were subjected to analysis of variance, and means were compared by Tukey's HSD test.

RESULTS

Images and chemical compositions using VP-SEM and tissue analysis for macro- and micro-elements

Multifaceted spherical and bladed aggregate crystals (druses) were observed in the cells of stems (Figure 1A, B) and leaves (Figure 1C) of *A. mosanensis* by VP-SEM. Druses were observed in cortical cells of the collenchyma tissue of the stem, but not in cells of the vascular bundles, pith, or periderm tissue of the stem, or in mesophyll cells surrounding the vascular bundles (Figure 1C). A few druses were observed in *A.* × *grandiflora* cells between the epidermis and the vascular bundles of the mid-vein of the leaf (Figure 1D). No druses or prismatic crystals were observed using VP-SEM in the epidermis in either species.

X-ray diffraction analysis for the chemical compositions of stems and leaves of *A. mosanensis* and *A.* × *grandiflora* detected Ca, Cl, K, Mg, P, S, and Si (Figure 2). Micro-analysis of cells from the leaves and stems of *A. mosanensis*, where no druses were present (Ce), indicated the presence of Ca, K, Mg, P, and S in leaves and Ca, K, and S in stems (Figure 2). Druses contained Mg in the leaves of both species, but only in the stems of *A. mosanensis* (Figure 2). Concentrations of K in druses in *A. mosanensis* [3.20 – 3.65% (w/w)] were higher than in cells [2.05 – 2.28% (w/w); Table I]. One exception where the Ca concentration was higher in the druse [20.60% (w/w)] than in the cell [8.58% (w/w)] was in the stems of *A.* × *grandiflora*. Mg concentrations in *A.*

Table I

Calcium (Ca), magnesium (Mg), and potassium (K) concentrations [% (w/w)] measured by quantitative X-ray diffraction in leaves and stems of A. mosanensis *and* A. × grandiflora

Species	Tissue	Cell or crystal[§]	Mg [%(w/w)]	Ca [%(w/w)]	K [%(w/w)]	Ca/Mg ratio
A. mosanensis	Leaf	Cell	0.16	2.29	2.07	14.3
		Crystal	0.26	6.82	6.85	26.2
	Stem	Cell	0.07	2.87	1.25	41.0
		Crystal	0.16	4.75	1.25	29.7
A. × *grandiflora*	Leaf	Cell	0.26	8.58	4.28	33.0
		Crystal	0.15	20.60	0.50	137.3
	Stem	Cell	0.91	1.67	0.29	1.8
		Crystal	0.21	0.50	0.48	2.4
Level of significance[‡]						
Species (SP)			*	*	*	–
Tissue (TS)			*	**	**	–
Cell *vs*. Crystal (CC)			**	**	**	–
SP × TS			*	**	ns	–
SP × CC			*	ns	**	–
TS × CC			*	*	ns	–
SP × TS × CC			ns	*	ns	–
HSD at $P \leq 0.01$			0.073	1.38	0.84	–

[§]Each X-ray analysis was performed by targeting a cell without any crystal (Cell), or the centre of a crystal.
Data for carbon, nitrogen, oxygen, silicon, phosphorus, sulphur, and chlorine are not presented. The totals would be 100% if the percentages (w/w) of these elements were added to the calcium, magnesium, and potassium data shown.
[‡]ns,*, **, not significant, or significant at $P \leq 0.05$, or $P \leq 0.01$, respectively by Tukey's HSD test.

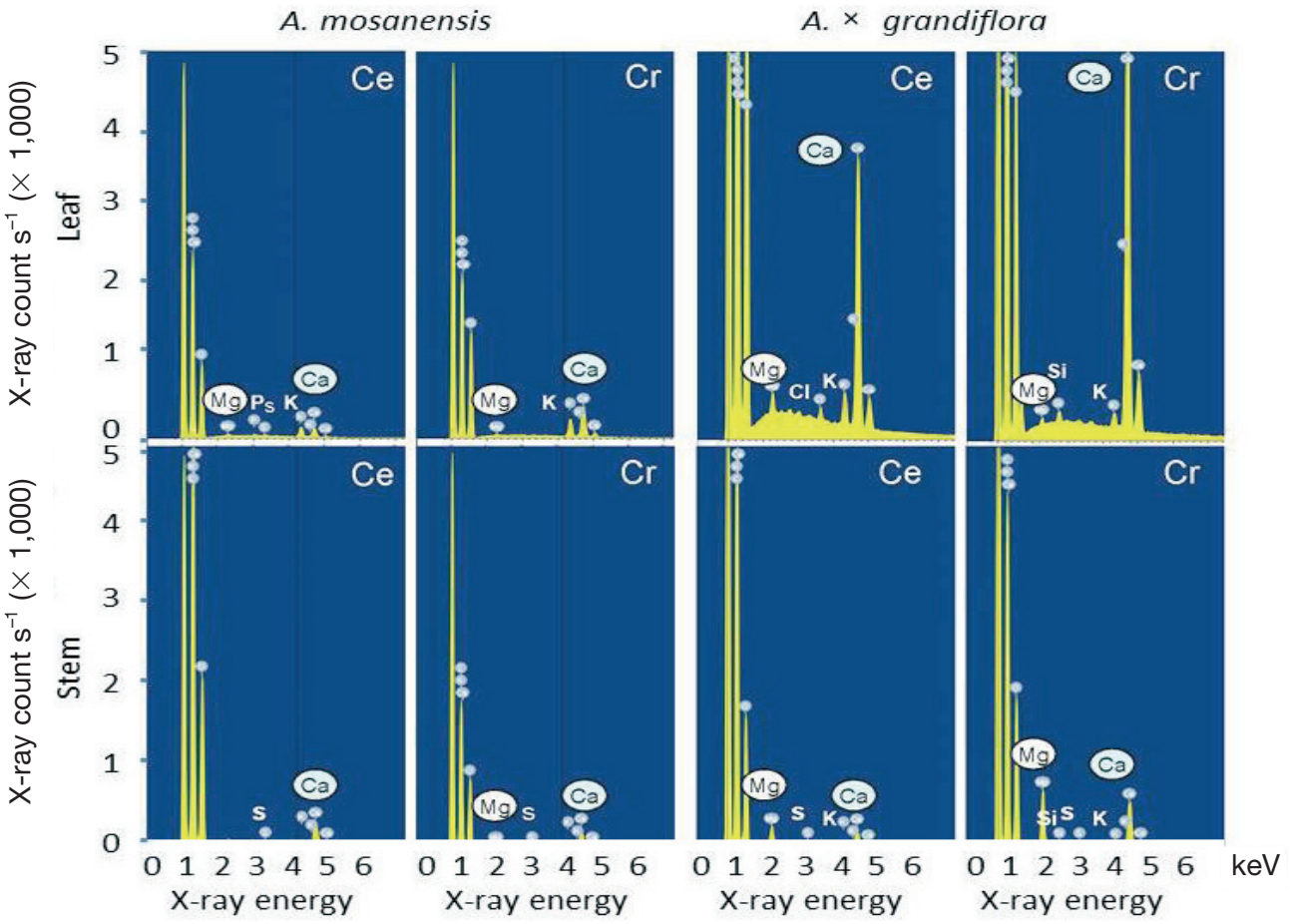

FIG. 2
Typical energy-dispersive X-ray spectroscopy spectra of cells of *A. mosanensis* or of *A.* × *grandiflora* without Ca oxalate crystals (Ce) or with Ca oxalate crystals (Cr). Large peaks on the left of each spectrum (mainly for carbon, hydrogen, and oxygen) are not labelled. X-ray counts for calcium (Ca), potassium (K), magnesium (Mg), sulphur (S), fluoride (F), and silicon (Si) are presented.

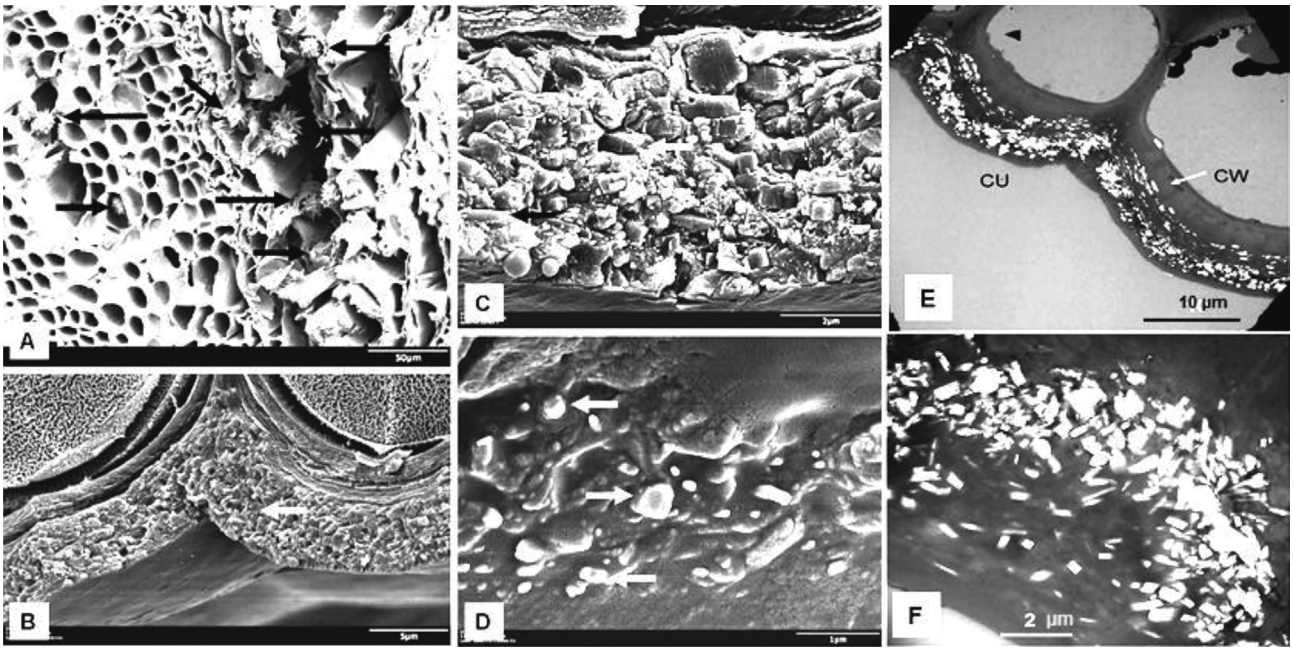

FIG. 3
Low temperature scanning (Panels A–D) and transmission (Panels E, F) electron microscope images of *A. mosanensis*. Numerous druses (arrows) are shown in the cortex (Panel A). Prismatic or sand crystals are shown in the cuticle of the lower epidermis (Panels B, C). Sand crystals are shown in the upper epidermis (Panel D). Numerous prismatic Ca oxalate crystals are shown in the cuticle (CU) adjacent to the cell wall (CW; Panel E). Magnified images of prismatic crystals are shown in Panel F. Scale bars = 50 µm (Panel A); 5 µm (Panels B and D); 2 µm (Panel C and F); and 10 µm (Panel E).

Table II
Analysis of leaf and stem cells of A. mosanensis *using an inductively coupled atomic emission spectrometer-IRIS plasma spectrometer*

Tissue	Potassium [%(w/w)][§]	Calcium [%(w/w)]	Magnesium [%(w/w)]
Leaf	0.14	2.13	0.17
Stem	0.15	0.49	0.08
Level of Significance[‡]	*	**	**
HSD at $P \leq 0.01$	0.09	0.04	0.02

[§]Data for other macro- and micro-elements are not presented.
[‡]*, **, Significant at $P \leq 0.05$, or $P \leq 0.0\,1\%$, respectively by Tukey's HSD test.

mosanensis cells were either low [0.07% (w/w)] or not detected (Figure 2). The Ca:Mg ratios in druses in leaves of *A. mosanensis* and *A.* × *grandiflora* were 26 and 137, respectively, which was higher than in cells without druses. However, the Ca:Mg ratio was lower in stems than in the leaves in both species.

X-ray diffraction analysis also showed that the weight percentages of Ca in roots and in calli at the base of stems in *A. mosanensis* cuttings ranged from 0.24 – 0.37% (w/w) and from 0.81 – 1.04% (w/w), respectively (data not shown). Tissue analysis showed that the concentrations [% (w/w)] of Ca and Mg were higher in leaves than in the stems of *A. mosanensis* (Table II). Ca and Mg concentrations ranged from 0.8 – 3.0% and from 0.2 – 8.8% (w/w), respectively, and were in the normal ranges recommended for floral and ornamental crops by the JR Peters Laboratory (Allentown, PA, USA).

Localisation, morphology, and growth of Ca oxalate crystals

Three major crystal shapes were observed in *A. mosanensis* using VP-SEM and TEM. Multi-faceted aggregate crystals with sharp points (druses) were seen in leaf cells surrounding the vascular bundles (Figure 3A). Large numbers of small angular crystals (sand crystals; Figure 3B – F), and block-like prismatic crystals were present as single or multiple crystals. Druses were observed in the cortical cells of *A.* × *grandiflora* leaves (Figure 4 A – C), however they were not observed in mesophyll cells, while sand crystals were not observed in the epidermis (Figure 4D). The sizes of the druses was approx. 20 μm × 15 μm (Figure 5A). The tips of the blades were generally sharp and pointed. A few tips (enclosed by dotted lines) were not sharp (Figure 5A). When the two circled areas in Figure 5B and 5C were enlarged, droplets (indicated with arrows) were observed.

A typical cortical parenchyma cell with intercellular spaces, cell walls, and a cell membrane, but without chloroplasts is shown in the TEM image of *A. mosanensis*

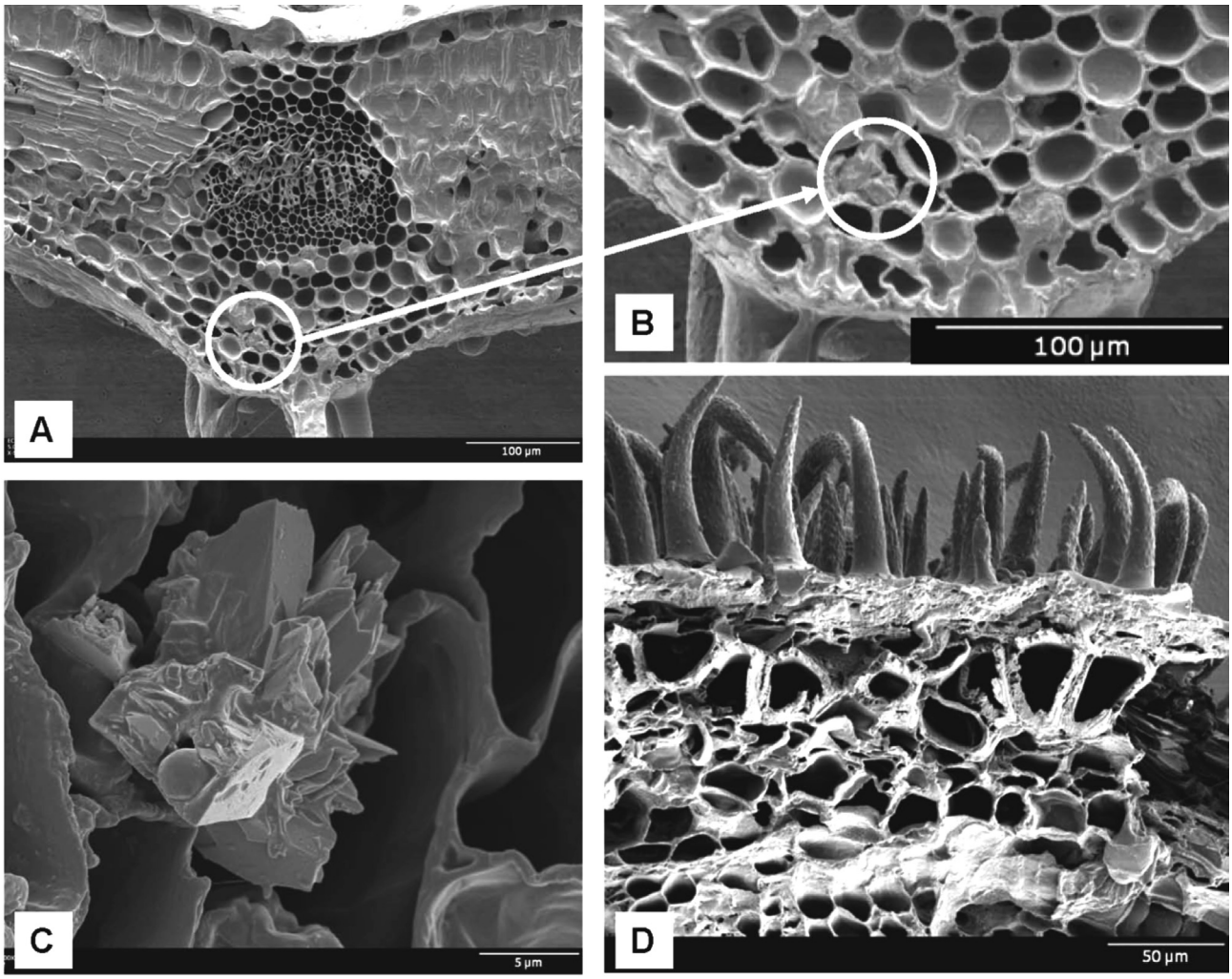

Fig. 4
Low temperature scanning electron microscope images of Ca oxalate crystals in the vacuole of a parenchyma cell (Panels A, B). Druses observed near the mid-vein of *A.* × *grandiflora* (Panel C), while crystals were not observed in the epidermis (Panel D) with numerous trichomes in *A.* × *grandiflora*. Scale bars = 100 μm (Panels A, B); 5 μm (Panel C); and 50 μm (Panel D).

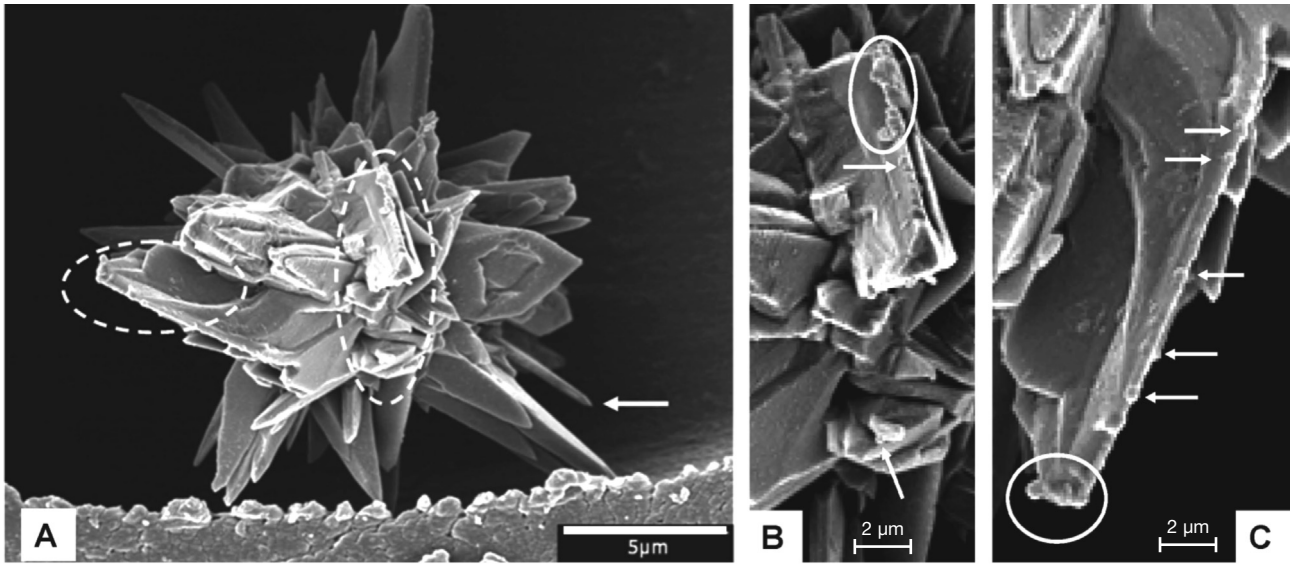

FIG. 5
Low temperature scanning electron microscope images of druses (calcium crystals) in the vacuole of a cortex cell of *A. mosanensis*. The areas enclosed by the dotted circles may indicate the formation of new crystals (Panel A). Close-up images (Panels B, C) of druses (Ca oxalate crystals) in the circled areas in Panel A. Arrows indicate semi-solid crystals that will develop to form solid calcium crystals. Scale bar = 5 µm (Panel A) and 2 µm (Panels B, C).

(Figure 6A). A single block-like prismatic crystal was present inside the chloroplast of a cortical parenchyma cell (Figure 6B), and two prismatic crystals were present outside the chloroplast (Figure 6C). An enlarged image of one prismatic crystal (approx. 1,500 µm in length and 830 µm in width; Figure 6D) showed three lines at both ends (numbered 1, 2, and 3) which might indicate that the crystal was growing.

DISCUSSION

This is the first report of the presence of Ca oxalate crystals of different morphologies and chemical compositions, and of the possible growth of Ca oxalate crystals in *Abelia*. Druses and prismatic crystals were visualised using VP-SEM, LT-SEM, and TEM. The crystals were identified as Ca oxalate, and contained mainly Si and Mg as minor elements.

Morphology and localisation of Ca oxalate crystals

More Ca oxalate crystals were observed in *A. mosanensis* than in *A.* × *grandiflora*, suggesting that crystal formation may be under genetic control (Ilarslan *et al.*, 2001). Although Ca oxalate crystals have been observed in many organs and tissues within plants, the site of crystal formation and distribution cannot be generalised, suggesting multiple origins (Franceschi and Nakata, 2005). Prismatic crystals, sand crystals, and druses with sharp and undamaged points on most facets (Arnott, 1982; Franceschi and Nakata, 2005) were observed in *Abelia* by VP-SEM, LT-SEM and TEM. Some facets of the druse had blunt ends which may have been damaged during sample preparation, as reported in *Peperomia* (Kuo-Huang *et al.*, 2007). Single, large, hexagon-shaped prismatic crystals were also found in the vacuoles or inside the chloroplasts of mesophyll cells which contained well-formed grana, as observed in *P. glabella* (Sw.) A. Dietr. (Kuo-Huang *et al.*, 2007), and also in the cytoplasm adjacent to the chloroplast in *A. mosanensis*. Although only one crystal was observed in each cell in *Peperomia*, two crystals were observed in *Abelia* in this study. Needle-shaped raphide crystals were not observed in our study. Numerous extremely small sand crystals were generally found in the cuticle of the epidermal layer of *A. mosanensis*.

Chemical composition of druse crystals

Based on X-ray dispersion elemental micro-analysis of druses using VP-SEM, we concluded that the crystals were Ca oxalate and contained Mg (i.e., Ca-Mg oxalate crystals), although the concentration of oxalic acid ($C_2H_2O_4$) was not analysed and the crystals were not subjected to HCl treatment in this study (*cf.* Franceschi and Nakata, 2005). Silicon was detected in the Ca oxalate crystals in *A.* × *grandiflora*, but not in *A. mosanensis*. We concluded that the crystals in *A. mosanensis* were Ca-Mg oxalate crystals, and were Ca-Mg-Si oxalate crystals in *A.* × *grandiflora*. Therefore, the druses were designated Ca oxalate crystals, or Ca oxalate containing Si. The prismatic crystals may also be designated Ca oxalate.

The detection of Si in *Abelia* is unique. Silicon was a contaminant from sand trapped on the roots of sweet potato [*Ipomoea batatas* (L.) Lam.; Schadel and Walter, 1980]. In our study, there was no possibile contamination by sand to produce the Si peak in the inter- and intra-cellular spaces of leaves and stems. The Si peak was from the crystals rather than from tissue devoid of crystals in *Acacia robeorum* Maslin (He *et al.*, 2012). However, the Si content was ≤ 0.09% (w/w) in all samples, thus the presence of Si in crystals may require further confirmatory analysis. Although three types of Ca oxalate crystals containing Ca alone, Ca-Si, or Mg-S-K have been reported in *Acacia robeorum* (He *et al.*, 2012), a K peak was observed in cells with or without crystals in *Abelia*. Therefore, we conclude that Ca oxalate crystals do not contain K in *Abelia*.

Growth of crystals

The formation of Ca oxalate crystals is considered to be under genetic control (Ilarslan *et al.*, 2001), but it is

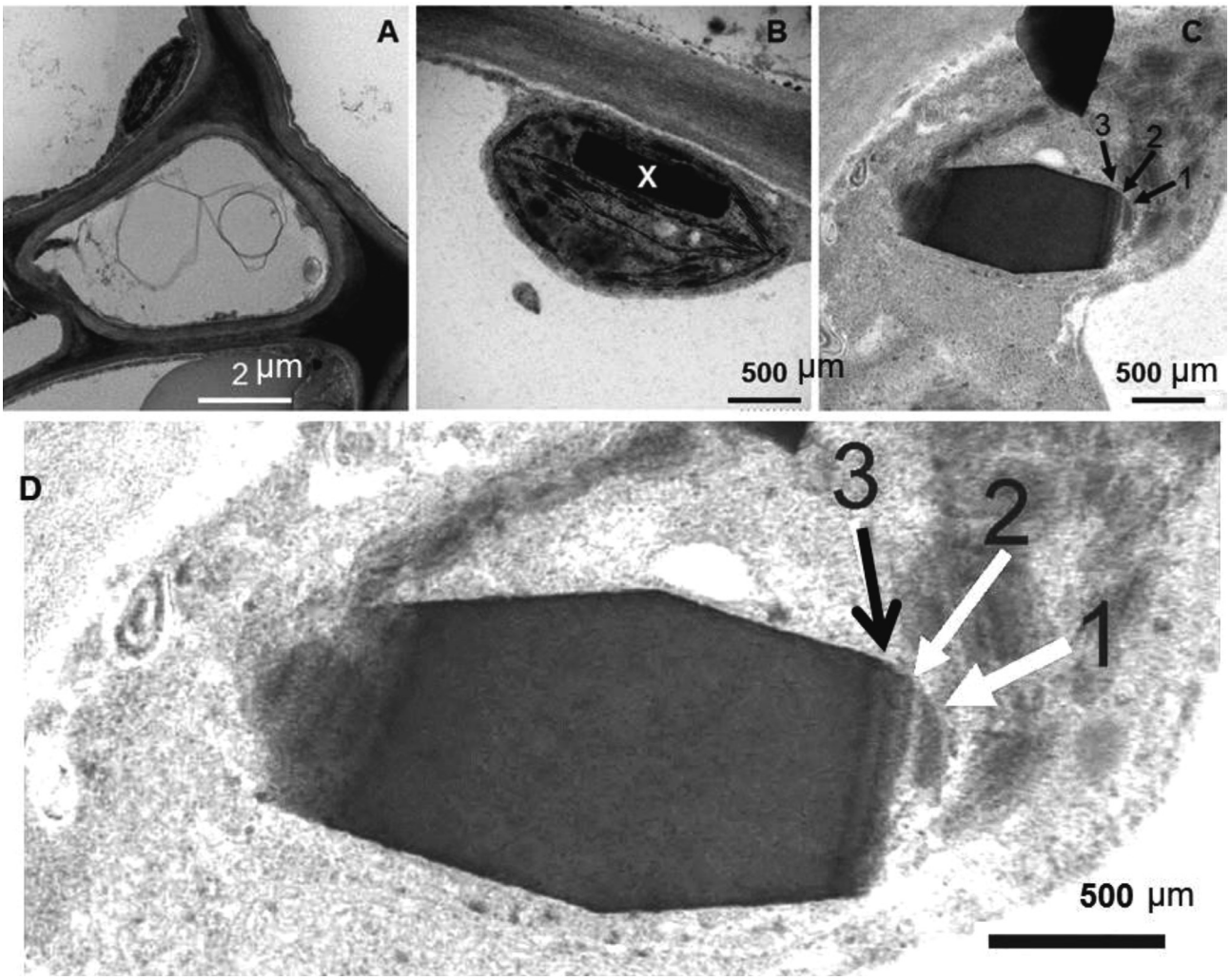

Fig. 6
Sub-cellular localisation of prismatic crystals revealed in transmission electron microscope images of cells in *A. mosanensis*. Typical cortex parenchyma cells showing intercellular spaces, cell walls, a cell membrane, and chloroplasts without Ca oxalate crystals (Panel A), a prismatic crystal marked with a cross inside the chloroplast (Panel B), a hexagonal prismatic crystal in the chloroplast showing the formation of three layers (Panel C), and a prismatic crystal enlarged to show the formation of the three layers (Panel D). Scale bars = 2 µm (Panel A) or 500 µm (Panels B–D).

not understood how the different crystal types are initiated, or how they expand. The development of crystals was related to the amount of Ca available in the soil in *Canavalla ensiformis* D.C. (Frank, 1972) or to the Ca concentration in leaves in *Arabidopsis* (Nakata, 2012). Calcium is translocated to leaves primarily via the xylem, resulting in higher Ca concentrations in the leaves than in the shoots of *A. mosanensis*. The elevated Ca concentration in leaves, as evidenced by foliar X-ray analysis, may contribute to the formation of Ca oxalate crystals. However, based on our tissue analysis of Ca concentrations, it is difficult to state that Ca concentration in the soil or in stems or in leaves affect the formation of Ca oxalate crystals. Nakata (2012) also concluded that there was no significant increase in Ca concentrations in crystal-forming plants, but that partitioning of the Ca present in the vacuole may facilitate crystal formation in *Arabidopsis*. However, the initiation of crystal formation is not yet clearly understood.

Once Ca oxalate crystals have been initiated, the crystals increased in size by the formation of flat crystalline lamellae, as reported in several cacti (Monje and Baran, 2002) or by the formation of facets as observed in *Peperomia* (Kuo-Huang *et al*., 2007). Semi-solid crystals, or true crystals that may result from Ca deposition at the ends of the facets radiating from the centre to form a solid Ca oxalate crystal were observed by LT-SEM (Figure 5). High magnifications of Ca oxalate crystals clearly showed the growth of druses (Figure 6). Different layers observed in the prismatic crystals suggested growth of the crystals. Calcium oxalate crystals, while not surrounded by a membrane, may be connected to the cell wall, suggesting that they are positioned inside cells devoid of cytoplasm (Ilarslan *et al*., 1999), as shown in the LT-SEM images in this study.

In conclusion, three morphologically distinct crystal types (prismatic crystals, sand crystals, and druses) were observed in the cells of two *Abelia* spp. No raphide crystals were observed in *Abelia*. Druses were composed of Ca oxalate, together with Mg and Si. The growth of prismatic crystals and druses may occur by the formation of crystalline lamellae or facets with the deposition of Ca, Mg, and/or Si. More species should be examined to see if Ca oxalate crystals are widely distributed in the genus *Abelia*.

Mention of a trade name, proprietary product, or specific equipment does not constitute a guarantee or warranty by the US Department of Agriculture and does not imply its approval to the exclusion of other products that may be suitable. We thank Drs. John Hammond and Roger Lawson for careful editing of the manuscript and Dr. L. Broadhurst for the X-ray dispersion data.

REFERENCES

Arnott, H. J. (1976). Calcification in higher plants. In: *The Mechanisms of Mineralization in Invertebrates and Plants*. (Watabe, N. and Wilbur, K.M., Eds.). South Carolina Press, Columbia University. Columbia, SC, USA. 55–73.

Arnott, H. J. (1982). Three systems of biomineralization in plants with comments on the associated organic matrix. In: *Biological Mineralization and Demineralization*. (Nancollas, G. H., Ed.). Springer Verlag, Berlin, Germany. 199–218.

Arnott, H. J. and Pautard, F. G. E. (1970). Calcification in plants. In: *Biological Calcification: Cellular and Molecular Aspects*. (Schraer, H., Ed.). Appleton-Century-Crofts, New York, NY, USA. 375–446.

Borchert, R. (1985). Calcium-induced patterns of calcium-oxalate crystals in isolated leaflets of *Gleditsia triacanthos* L. and *Albizia julibrissin* Durazz. *Planta*, **165,** 301–310.

Cuadra, V. P., Cambi, V. N., Rueda, M., De Los, Á. and Calfuán, M. L. (2012). Consequences of the loss of traditional knowledge: The risk of injurious and toxic plants growing in kindergartens. *Ethnobotany Research & Applications*, **10,** 77–94.

Doaigey, A. R. (1991). Occurrence, type, and location of calcium oxalate crystals in leaves and stems of 16 species of poisonous plants. *American Journal of Botany*, **78,** 1608–1616.

Franceschi, V. R. (1984). Developmental features of calcium oxalate crystal sand deposition in *Beta vulgaris* L. leaves. *Protoplasma*, **120,** 216–223.

Franceschi, V. R. (1989). Calcium oxalate formation is a rapid and reversible process in *Lemna minor* L. *Protoplasma*, **148,** 130–137.

Franceschi, V. R. and Horner Jr., H. T. (1980). Calcium oxalate crystals in plants. *Botanical Review*, **46,** 361–427.

Franceschi, V. R. and Nakata, P. A. (2005). Calcium oxalate in plants: Formation and function. *Annual Review of Plant Physiology*, **56,** 41–71.

Frank, E. (1972). The formation of crystal idioblasts in *Canavalia ensiformis* D.C. at different levels of calcium supply. *Zeitschrift für Phlanzenphysiologie*, **67,** 350–350.

Frey-Wyssling, A. (1981). Crystallography of the two hydrates of crystalline calcium oxalate in plants. *American Journal of Botany*, **68,** 130–141.

Gallaher, R. N. and Jones, J. B. J. (1976). Total, extractable, and oxalate calcium and other elements in normal and mouse ear pecan tree tissues. *Journal of the American Society for Horticultural Science*, **101,** 692–696.

He, H., Bleby, T. M., Veneklass, E. J., Lambers, H. and Kuo, J. (2012). Morphologies and elemental compositions of calcium crystals in phyllodes and branchlets of *Acacia robeorum* (Leguminosae: Mimosoideae). *Annals of Botany*, **109,** 887–896.

Horner Jr., H. T. and Wagner, B. L. (1980). The association of druse crystals with the developing stomium of *Capsicum annuum* (Solanaceae) anthers. *American Journal of Botany*, **67,** 1347–1360.

Horner Jr., H. T. and Franceschi, V. R. (1981). The use of a tissue culture system as an experimental approach to the study of plant crystal cells. *Scanning Electron Microscopy*, **3,** 245–249.

Ilarslan, H., Horner. H. T. and Palmer, R. G. (1999). Genetics and cytology of a new male-sterile, female-fertile soybean mutant. *Crop Science*, **39,** 58–64.

Ilarslan, H., Palmer, R. G. and Horner, H. T. (2001). Calcium oxalate crystals in developing seeds of soybean. *Annals of Botany*, **88,** 243–57

Kirkby, E. A. and Pilbeam, D. J. (1984). Calcium as a plant nutrient. *Plant, Cell and Environment*, **7,** 397–405.

Kram, A. M., Oostergetel, G. T. and Van Bruggen, E. F. J. (1993). Localization of branching enzyme in potato tuber cells with the use of immune-electron microscopy. *Plant Physology*, **101,** 237–243.

Kuo-Huang, L-L., Ku, M. S. B. and Franceschi, V. R. (2007). Correlations between calcium oxalate crystals and photosynthetic activities in palisade cells of shade-adapted *Peperomia grabella*. *Botanical Studies*, **48,** 155–164.

Lee, J. S. and Roh, M. S. (2001). Influence of frozen storage duration and forcing temperature on flowering of oriental hybrid lilies. *HortScience*, **36,** 1053–1056.

Libert, B. and Franceschi, V. R. (1987). Oxalate in crop plants. *Journal of Agricultural and Food Chemistry*, **35,** 926–938.

Monje, P. V. and Baran, E. J. (2002). Characterization of calcium oxalates generated as biominerals in cacti. *Plant Physiology*, **128,** 707–713.

Nakata, P. A. (2012). Engineering calcium oxalate crystal formation in *Arabidopsis*. *Plant Cell Physiology*, **53,** 1275–1282.

Roh, M. S., Bauchan, G. R. and Huda, M. S. (2012). Physical and chemical properties of biobased plastic resins containing chicken feather fibers. *Horticulture, Environment and Biotechnology*, **53,** 72–80.

Schadel, W. E. and Walter Jr., W. M. (1980). Calcium oxalate crystals in the roots of sweet potato. *Journal of the American Society for Horticultural Science*, **105,** 851–854.

Scurfield, G., Michell, A. J. and Silva, S. R. (1973). Crystals in woody stems. *Botanical Journal of the Linnean Society*, **6,** 277–289.

Spurr, A. R. (1969). A low-viscosity epoxy resin embedding medium for electron microscopy. *Journal of Ultrastructure Research*, **26,** 31–43.

SAS. (2002). *SAS Proprietary Software. Version 9.00*. SAS Institute Inc., Cary, NC, USA.